JOURNAL OF SOLID STATE CHEMISTRY **132,** 163–172 (1997)
ARTICLE NO. SC977437

Synthesis, Structural, and Magnetic Characterization of New $Hg_2Ba_2LnCu_2O_{8-\delta}$ Phases with Ln = Nd–Gd, Dy–Lu

S. M. Loureiro,[1] C. Chaillout, E. Gautier, and J. J. Capponi

Laboratoire de Cristallographie, CNRS, BP 166, 38042 Grenoble Cedex 09, France

P. Toulemonde

CRTBT, CNRS, BP 166, 38042 Grenoble Cedex 09, France

E. V. Antipov

Department of Chemistry, Moscow State University, 119899 Moscow, Russia

J. L. Tholence

LEPES, CNRS, BP 166, 38042 Cedex 09, France

and

M. Marezio

Maspec-CNR, Via Chiavari 18/A, 43100 Parma, Italy

Received April 16, 1997; accepted April 21, 1997

New phases of general formula $Hg_2Ba_2LnCu_2O_{8-\delta}$ with Ln = Nd–Gd, Dy–Lu were synthesized by high-pressure, high-temperature technique. All the compounds crystallize in space group I 4/m m m and the lattice parameters were found to increase with the ionic radii, ranging from a=3.8460(3) Å, c=28.853(3) Å for Lu up to a=3.9021(3) Å, c=28.986(3) Å for Nd. Hg-2212 phases were not obtained with La, due to the high ionic radius of La^{3+}, or with cations having possible valences higher than (+3), such as Tb, Pr, and Ce. Energy dispersive spectroscopy (EDS) analysis performed on samples with Lu, Yb, Er, and Gd showed significant Hg-deficiency as well as rare earth overstoichiometry. This allows us to suggest that lanthanide cations partially substitute for Hg and that these phases are better described as $(Hg,Ln)_2Ba_2LnCu_2O_{8-\delta}$. The substitution rate depends on the ionic radii of the lanthanide cation, varying between 25% for Lu (0.977 Å) or Er (1.004 Å) to 15% for Gd (1.053 Å). In the case of Nd-sample it was found that Nd does not replace Hg but Ba instead. The large ionic radius of Nd (1.109 Å) can probably account for this effect and this phase would be described as $Hg_2(Ba,Nd)_2NdCu_2O_{8-\delta}$. The susceptibility of Sm, Eu, Dy, and Ho samples exhibits a sharp cusp at a temperature T_L between 25 and 28 K. These temperatures are attributed to the antiferromagnetic binding of Cu spins, because they are too high to be due to rare earth ordering. Specific heat and neutron diffraction experiments are planned to establish an eventual cooperative ordering of Cu and rare earth moments. © 1997 Academic Press

[1]To whom correspondence should be addressed. Fax: (33) 76.88.10.38. E-mail: loureiro@labs.polycnrs.gre.fr.

INTRODUCTION

The first Hg-1212 phases were synthesized by Putilin *et al.* (1). They were actually the second member of the homologous series $HgBa_2R_{n-1}Cu_nO_{2n+2+\delta}$ [Hg-12($n-1$)n]. These authors prepared those with R = yttrium and lanthanide cations such as La, Nd, Eu, Gd, and Dy. Recently, other substitutions throughout the lanthanide series including Ho, Er, Tm, Yb (2), and Sm (3) were also carried out. Despite the absence of superconductivity in these phases, this work was a major breakthrough since it led to the synthesis of $HgBa_2CuO_{4+\delta}$ in 1993, which was the first high-T_c Hg-based superconductor (T_c = 94 K) (4). Subsequently, the synthesis of Hg-1212 and Hg-1223 with Ca instead of R led to the record of superconductivity (T_c = 133 K) for the third member of the homologous series (5). From the structural point of view, the arrangement is

0022-4596/97 $25.00

very similar to that of Tl-12$(n-1)n$ series. However, thallium was found to form not only monolayer (TlO) charge reservoirs, but also bilayer $(TlO)_2$ ones, giving rise to the homologous series Tl-22$(n-1)n$. The same was not found right away for mercury, until in 1994 when a new Hg-based Cu-mixed oxide containing double $(HgO)_2$ layers was synthesized. The stacking would then be:

$$-(MO_\delta)-(MO_\delta)-(BaO)-(CuO_2)-(M'-CuO_2)_{n-1}-(BaO)-$$
$$-(MO_\delta)-(MO_\delta)-$$

The first synthesis done with praseodymium (6), $(Hg_{1.5}Pr_{0.3}Cu_{0.2})Ba_2PrCu_2O_{8-\delta}$, and yttrium (7, 8), $Hg_2Ba_2YCu_2O_{8-\delta}$, led to nonsuperconducting phases. Superconductivity was induced by heterovalent substitution (7, 8) of Y^{+3} by Ca^{+2}, as in $Hg_2Ba_2(Ca,Y)Cu_2O_{8-\delta}$ (7). This motivated us to perform a systematic study of new phases in the Hg-2212 system in which Y is substituted by rare earth elements. We report here the synthesis of new Hg-2212 phases with Ln = Lu, Yb, Tm, Er, Ho, Dy, Gd, Eu, Sm, and Nd. These new phases were characterized by X-ray powder diffraction, electron microscopy, EDS analysis and ac magnetic susceptibility.

EXPERIMENTAL

A set of precursors of nominal stoichiometry $Ba_2LnCu_2O_y$ (Ln = Lu, Yb, Tm, Er, Ho, Dy, Tb, Gd, Eu, Sm, Nd, Pr, Ce, and La) was prepared by mixing high-purity oxides BaO_2, [Ln_2O_3 (for Lu–Nd, La), Pr_6O_{11}, or CeO_2] and CuO in an agate mortar, placing them in a tubular furnace at 835°C under oxygen for 24 h with one intermediate grinding and quenching. After this process all the oxides present in the precursors had the lanthanides in their highest valence with the exception of Tb, where mixed valence (+3, +4) oxides were present. These precursors were subsequently mixed with 1.75 HgO to produce $Hg_{1.75}Ba_2LnCu_2O_y$ nominal stoichiometries.[2] The mixture was placed in a gold capsule appropriated for high-pressure, high-temperature synthesis which was carried out at 18 kbar/920°C/2 h.

X-ray powder patterns were collected within $10^\circ \le 2\theta \le 90^\circ$, with a Siemens D5000 powder diffractometer in transmission mode, equipped with a Ge monochromator placed on the primary beam (Cu$K\alpha_1$ radiation, $\lambda = 1.54056$ Å), a rotating sample, and a mini-PSD. The electron microscopy study as well as the EDS microanalysis were performed on a Philips CM300 microscope operating at 300 kV ad equipped with a Kevex sigma analyzer. The powders were ground in acetone in an agate mortar and the crystallites were recovered from the suspension on a holey carbon grid.

[2]The nominal stoichiometry of $Hg_{1.75}Ba_2LnCu_2O_{8-\delta}$ was optimized during the synthesis of yttrium-based Hg-2212 phases. Samples with nominal stoichiometries superior to 1.75 in Hg have always shown an excess of HgO by X-ray powder diffraction. Samples with nominal stoichiometries inferior to this value have shown reflections of the Hg-1212 phases.

DISCUSSION

X-Ray Powder Diffraction

The X-ray powder patterns of the obtained phases are shown in Figs. 1a and 1b. The Hg-22Ln2 phases were obtained with different purity rates. Samples with smaller rare earth cations such as Lu, Yb, and Tm have produced $\approx 80\%$ Hg-22Ln2 phases while those with larger lanthanides reached even up to 95%. Although a nominal mercury stoichiometry of only 1.75 was used, all the samples still contained traces of mercury oxide as impurity. The amount of HgO increases when the samples contain smaller lanthanide cations. Other types of impurities commonly found in the samples were also Ln_2BaCuO_5 as well as traces of CuO.

On the other hand, and although 2212 phases with Pr have already been reported (5), such as $(Hg_{1.5}Pr_{0.3}Cu_{0.2})Ba_2PrCu_2O_{8-\delta}$, whenever the lanthanide had a mixed valence $Ln^{+3,+4}$, as in Tb, Pr, or Ce, 2212 phases were not found to form at our synthesis conditions. This is easily explained since our synthesis was done in oxidizing conditions, where the lanthanide cannot be reduced to the (+3) formal valence, necessary for the cations to be located between the two (CuO_2) layers. A more reduced precursor would increase the probability of synthesizing 2212 phases with these cations. However, as in the case of 123 phases, this position (between two CuO_2 layers) is not suitable for a (+4) cation.

The La-based Hg-2212 phase was not obtained at our synthesis conditions. The sample contained instead a $La_{2-x}Ba_xCuO_{4+\delta}$ superconducting phase, other unknown impurities, and HgO and CuO.

All the synthesized Hg-22Ln2 phases are tetragonal, space group $I\,4/m\,m\,m$ and their lattice parameters varied from $a = 3.8460(3)$ Å and $c = 28.853(3)$ Å for lutetium to $a = 3.9021(3)$ Å and $c = 28.986(5)$ Å for neodymium. An ionic radius variation of 0.132 Å [0.977 Å (Lu) to 1.109 Å (Nd)] corresponds to a cell volume change of 14.56 Å^3 [426.79 Å^3 (Lu) to 441.35 Å^3 (Nd)] (C.N. VIII). In Fig. 2a we can see the variation of lattice parameter a as a function of the ionic radius of the rare earth. This variation is linear and agrees well with the variation of the rare earth's ionic radius. The variation of the lattice parameter c (Fig. 2b), although not being monotonous, presents also a general increasing variation with the rare earth ionic radius. There are, however, two dissonant points, 2212-Yb and Nd, where the c-parameter lies out of the guide line.

The absolute variation of the lattice parameters is obviously much more important for c reaching 0.196 Å [Nd–Yb] or 0.133 Å [Nd–Lu], while that for a is only of 0.0561 Å [Nd–Lu].

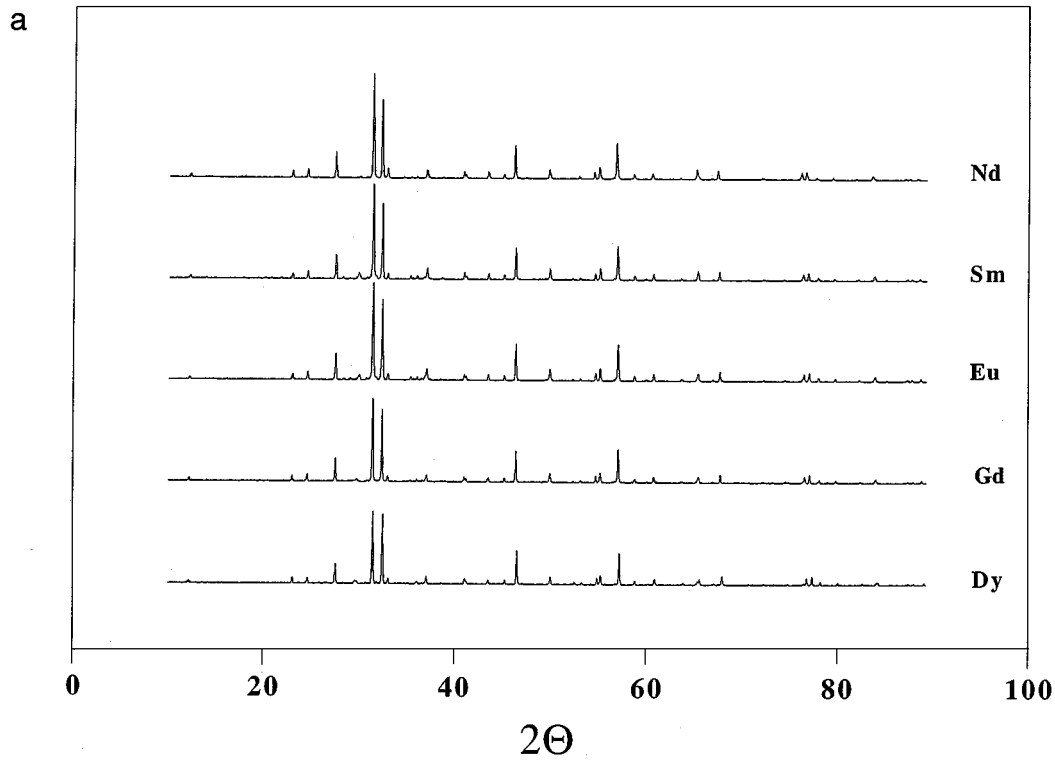

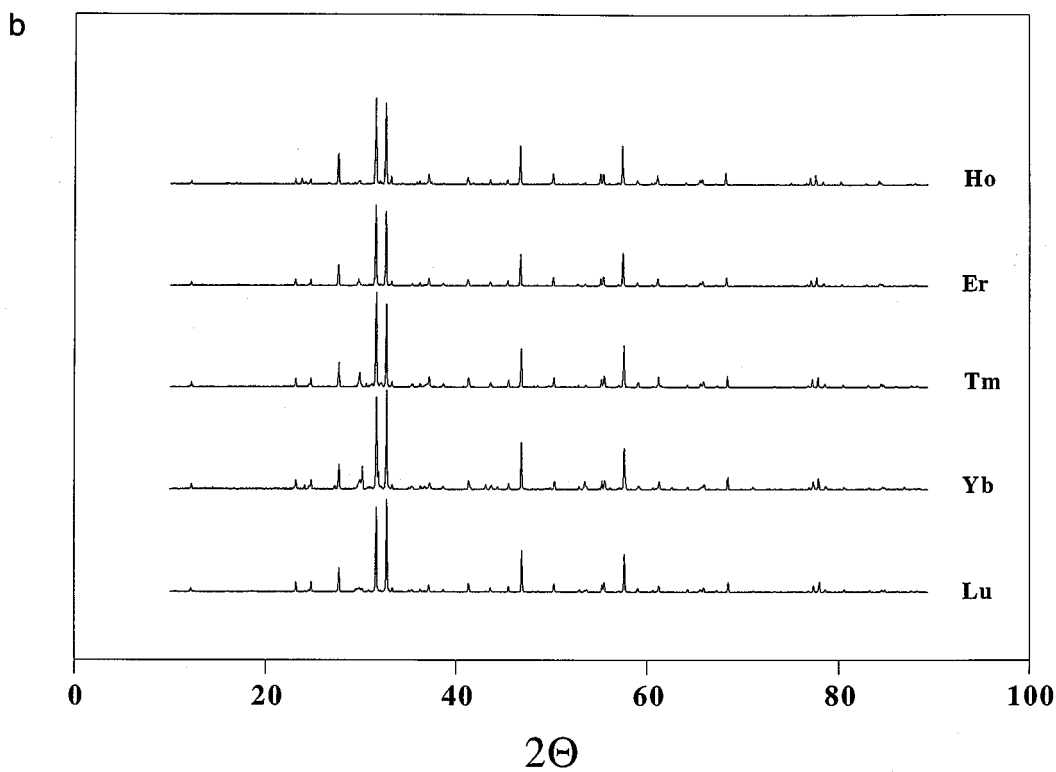

FIG. 1. (a and b) X-ray powder pattern of the 10 new Hg-22*Ln*2 synthesized phases.

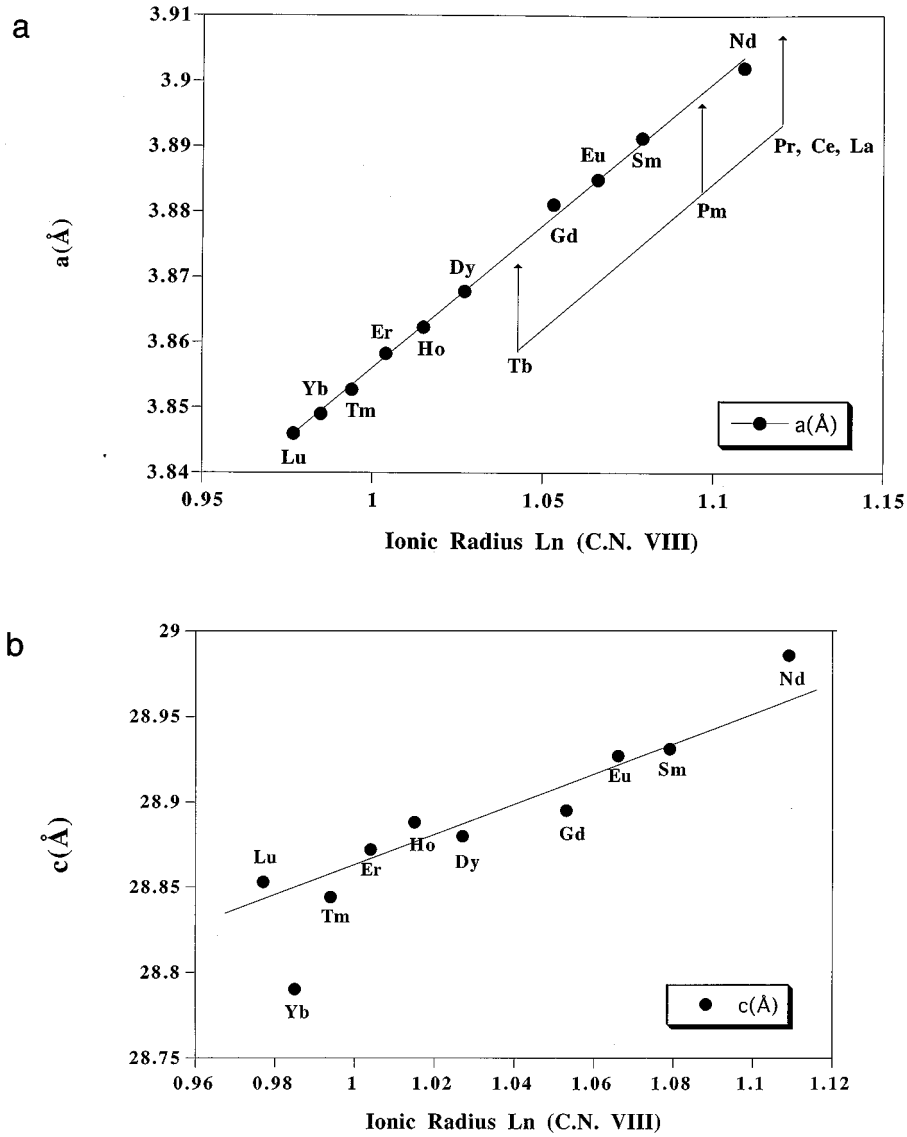

FIG. 2. (a) Lattice parameter a of the Hg-22*Ln*2 phases as a function of the ionic radius of the rare earth. (b) Lattice parameter c of the Hg-22*Ln*2 phases as a function of the ionic radius of the rare earth. (c) Cell volume V of the Hg-22*Ln*2 phases as a function of the ionic radius of the rare earth.

When compared to the Hg-12*Ln*2 series, we can see that the lanthanum substituted phase was found to form in the monolayer-Hg system (1) but not in the bilayer-Hg system and that the absolute variation of both lattice parameters a and c is, respectively, of 0.058 Å [Nd–Yb] and 0.094 Å [Nd–Yb]. These values are approximately the same as those found for the Hg-22*Ln*2 series since in this case the I-centered structure doubles the c-parameter which would mean $a\ \Delta c \approx 0.19$.

Transmission Electron Microscopy and EDS Analysis

Samples of 2212-Lu, Yb, Er, Gd, and Nd were analyzed by transmission electron microscopy. The phases were found to be well crystallized. As an example, Fig. 3 shows an electron diffraction pattern taken along the ⟨100⟩ zone axis for a 2212-Yb crystalline. Ten to 20 crystallites were analyzed by EDS for each sample. The average ratios Hg/Cu, Ba/Cu, *Ln*/Cu, (Hg + *Ln*)/Cu, (Ba + *Ln*)/Cu as well as the deduced chemical formula are reported in Table 2. Their variations as a function of the ionic radius of the lanthanide is shown in Figs. 4a and 4b (see also Table 1).

For each crystallite, the chemical formula was deduced in two different ways: either by assuming that the total number of cations in the formula was 7, which supposes that no partial substitution of Hg by carbonate groups takes place, or by stating that the number of Cu cations is equal to 2. This implies that there is no partial replacement of Hg by

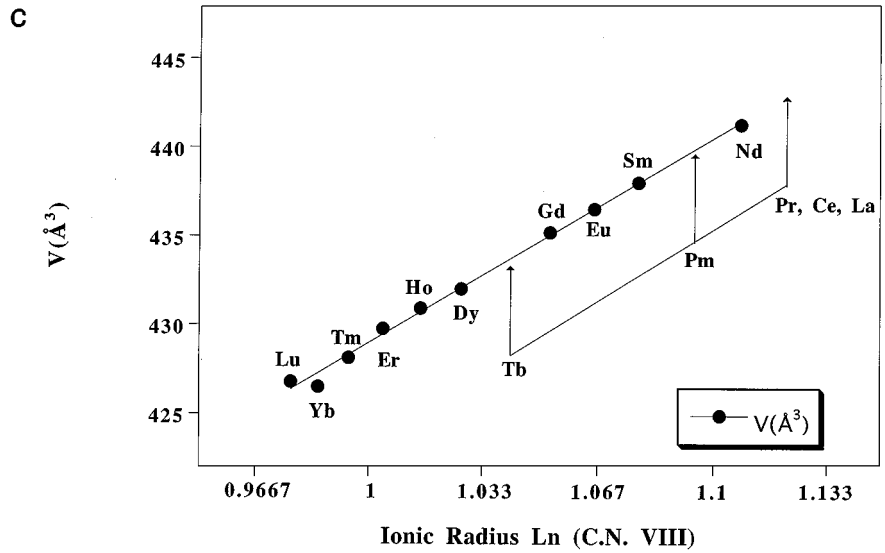

FIG. 2—*Continued*

Cu. Both methods gave similar chemical formulae, within standard deviations.

In all samples, the amount of rare earth appears to be larger than 1, as would be expected from a *Ln*-2212 formula, and the excess of rare earth seems to increase slightly as the ionic radius of the lanthanide decreases from Nd to Lu. On the other hand, the Hg/Cu ratio decreases from 0.92(9) in the case of Nd-2212 ($\approx$ full occupancy of the site by Hg) to 0.75 (5) for Lu. These two results can be interpreted as the partial substitution of the rare earth cations on the Hg site. This is valid for Lu, Yb, Er, and Gd samples and is supported by the fact that the (Hg + *Ln*)/Cu ratio is constant and very close to 1.5. On the other hand, the (Ba + *Ln*)/Cu ratio decreases from Lu to Gd but is always above 1.5, with a Ba/Cu ratio constant and equal to 1.

The case of Nd-2212 samples seems different: the Ba/Cu ratio is lower than 1, whereas the Hg/Cu one is equal to 1 within one standard deviation and the (Ba + Nd)/Cu one

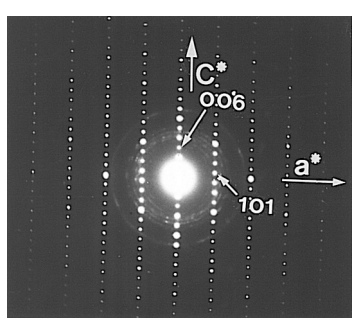

FIG. 3. Electron diffraction pattern of an 2212-Yb crystallite taken along the ⟨100⟩ zone axis.

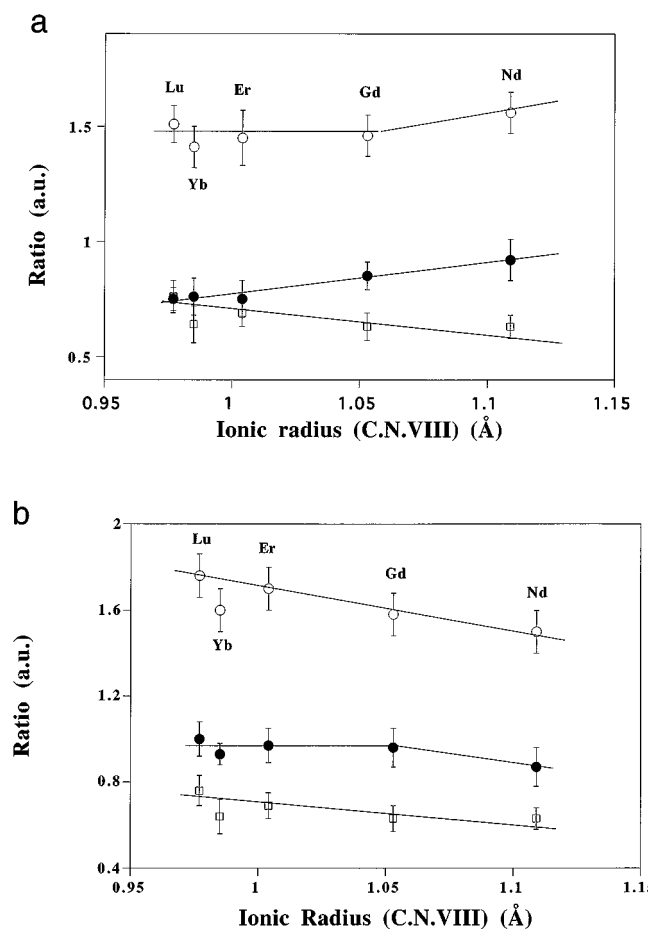

FIG. 4. Cation ratios as determined by EDS analysis for Lu, Yb, Er, Gd, and N Hg-22*Ln*2 phases: (a) Hg/Cu (black circles), (Hg + *Ln*)/Cu (white circles), *Ln*/Cu (white squares); (b) Ba/Cu (black circles), (Ba + *Ln*)/Cu (white circles), *Ln*/Cu (white squares).

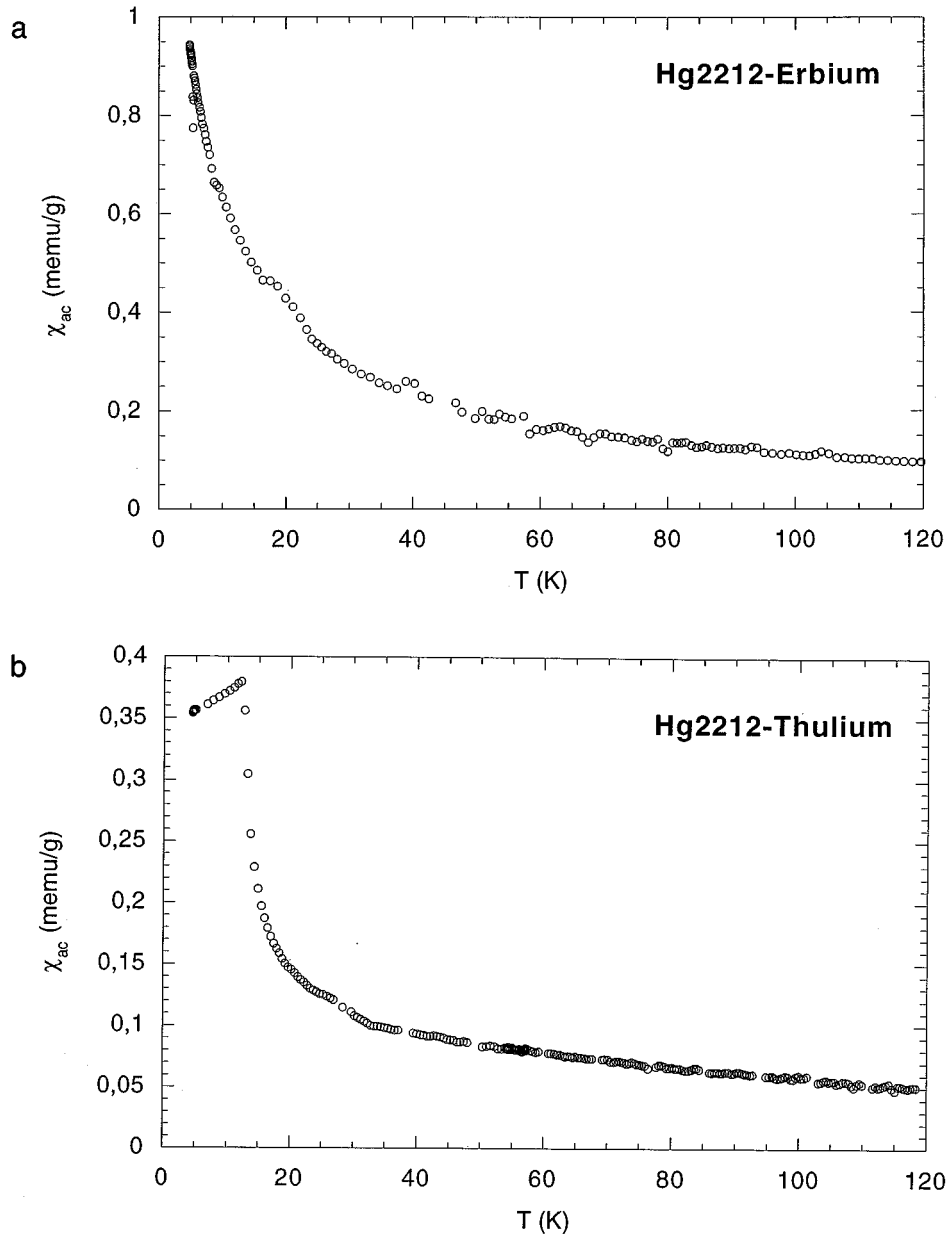

FIG. 5. Real part of the a.c. susceptibility of the 2212-*Ln* samples with Ln = (a) Er, (b) Tm, (c) Gd, (d) Sm. (e) Real and imaginary parts of the a.c. susceptibility of the 2212-Ho.

is equal to 1.5. This would imply that part of the Nd cations replace Ba and not Hg.

We have previously mentioned that the *c*-axis parameter of the Yb-2212 sample was slightly out of the guide line drawn for all samples. Here also, it seems that the Yb/Cu, (Hg + Yb)/Cu and (Ba + Yb)/Cu ratios for this sample are slightly below the line joining the values obtained for Lu, Er, and Gd samples. However, no other element such as Sr (a possible contaminant in Ba-based reactants such as BaO_2 and whose smaller size may explain the shorter *c*-parameter) that could replace Ba has been detected on the EDS spectra. One explanation may be that the Hg vacancies are not fully compensated by Yb cations but partially by carbonate groups. The presence of C–O bonds which are shorter than the Hg–O or Yb–O ones may account for the shorter *c* axis parameter.

MAGNETIC CHARACTERISATION

The a.c. susceptibility of the Hg-22*Ln*2 samples was measured with a mutual inductance bridge working at 119 Hz with an a.c. field of 1.2 Oe on finely grinded powder. As in

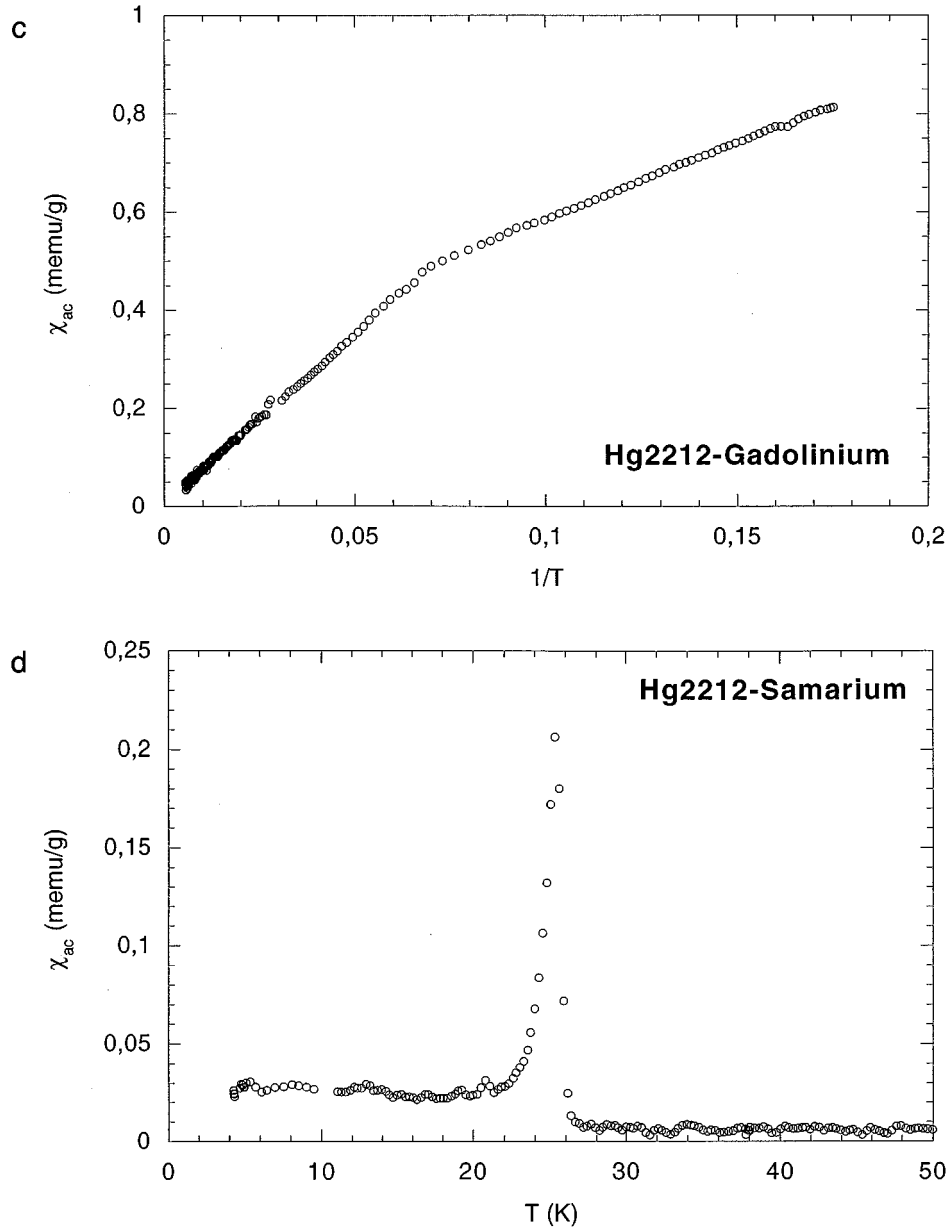

FIG. 5—*Continued*

the case of $Hg_{2-x}(Cu,Pr)_xBa_2PrCu_2O_{8-\delta}^6$, no superconductivity was observed down to 4.2 K

The lanthanide ions Ln^{3+} have the (Kr)4f^{n}5$s^2$5p^6 electronic structure and their magnetic properties are due to 4*f* electrons. Most of them are paramagnetic, whereas La^{3+} and Lu^{3+} have no magnetic moment and are diamagnetic. The effective magnetic moments and Curie–Weiss temperatures θ (K) are given in Table 3 for both Hg-22*Ln*2 samples and free lanthanide ions. As can be noticed, the total effective moments of Hg-22*Ln*2 samples determined experimentally are close to the expected values for the free Ln^{3+} ions.

For the 2212-Lu sample, no particular magnetic features were detected and the a.c. susceptibility is nearly constant (0.037 memu/g). On the other hand, Hg-22*Ln*2 samples, with *Ln* = Nd, Er, and Yb, present a Curie–Weiss dependence down to 4.5 K with negative $\theta = -4.4$, -9.5, and -4.4. K, respectively (Fig. 5a). The 2212-Tm sample presents a Curie–Weiss behavior above 28 K with a θ of ≈ -50.7 K and a ferromagnetic (or ferrimagnetic) transition below 12 K with a spontaneous magnetization due to an ordered spin state is observed (Fig. 5b). The Gd-compound also follows a Curie–Weiss law, but with two different slopes depending on the temperature range: above

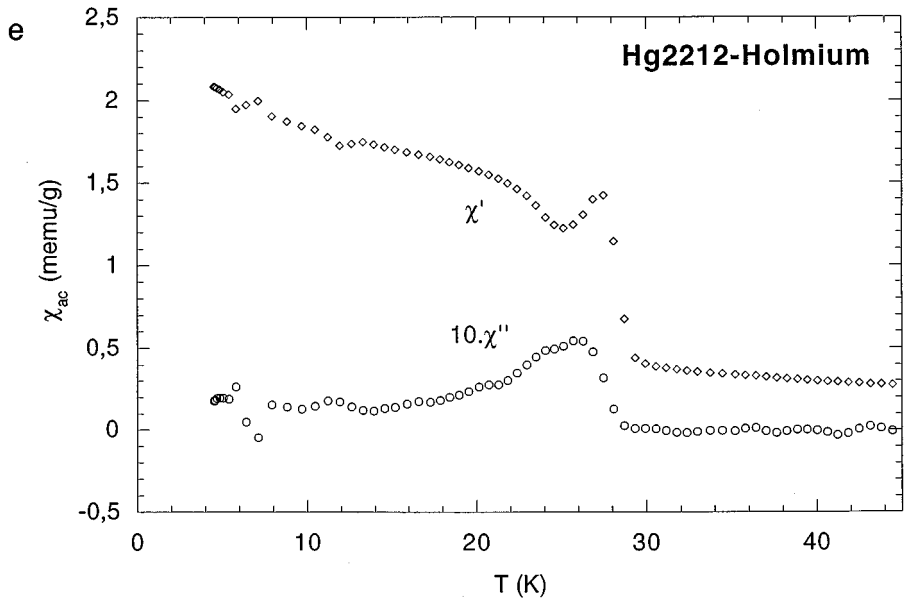

FIG. 5—*Continued*

12 K, the Curie-constant is 3.1 and below 12 K it is 6.7 (Fig. 5c). For Ln = Sm, Eu, Dy, and Ho, a particular behavior was observed. The a.c. susceptibility, χ', exhibits a sharp cusp at a temperature T_L between 25 and 28 K for the four compounds. A cusp in the imaginary part, χ'', of the susceptibility, is also observed at the same temperature. Below T_L the a.c. susceptibility falls down to a value which, in the case of Sm, Eu, Dy is larger than the value above T_L but approximately with the same thermal dependence. For instance, the susceptibility, which is almost temperature independent for Sm and Eu, remains also temperature independent below T_L (Fig. 5d), but increased by a constant value. In the case of Dy, the high temperature susceptibility follows a law $\chi' = \chi_0 + C/(T - \theta)$ with a negative $\theta = -6.6$ K. Below T_L, χ_0 has increased by a constant value of 0.1 memu/g. These experiments confirm that only a constant term is added to the susceptibility, independently of the magnetic (or nonmagnetic) state of Sm, Eu, or Dy. The holmium sample shows more clearly the effect of the ferromagnetic-like interactions at $T_L = 27$ K (Fig. 5e). Again, a constant increase of χ' is observed when the temperature goes below T_L. However, the increase is much larger than for Sm, Eu, and Dy.

In the case of the Ho sample, χ'' starts to increase at the same temperature as χ', it reaches a maximum below T_L, at about the temperature where $d\chi'/dT > 0$ is maximum. This indicates that the decrease of χ' and the maximum of χ'' are caused by losses due to some magnetic viscosity.

To better understand what happens around T_L we have measured the magnetization of the 2212-Ho sample between 0 and 14 T and in the temperature range of 5–50 K. The high temperature and high field parts of the magnetization can be fitted with a Brillouin function with the same parameter (Fig. 6a). However, below ≈ 50 K, we have to add a constant value, M_S, in order to get a correct representation of the magnetisation curves above 0.5 T. This indicates that we have a fraction of the magnetisation, M_S, which appears at low temperature and is easily saturated (below 0.5 T). A plot of M_S versus T (Fig. 6b) indicates that M_S falls by a factor of 10 between 5 and 27 K. This small M_S is the only indication in the magnetization corresponding to the susceptibility anomaly observed at 27 K. Although M_S does not seem to disappear abruptly above 27 K, which may be due to the uncertainty in the Brillouin fits, it is reasonable to associate M_S to the susceptibility increase below T_L.

TABLE 1
Ionic Radius of the Ln^{3+} Cation (CN VIII), Lattice Parameters, and Cell Volume of the Hg-22Ln2 Synthesized Phases

Ln	Ionic radius (Å)	*a* (Å)	*c* (Å)	*V* (Å^3)
Lu	0.977	3.8460(3)	28.853(3)	426.79
Yb	0.985	3.849(1)	28.79(1)	426.52
Tm	0.994	3.8527(3)	28.844(4)	428.14
Er	1.004	3.8582(4)	28.872(4)	429.78
Ho	1.015	3.8623(4)	28.888(4)	430.93
Dy	1.027	3.8678(4)	28.880(5)	432.04
Gd	1.053	3.8811(3)	28.895(3)	435.24
Eu	1.066	3.8849(5)	28.927(4)	436.57
Sm	1.079	3.8913(4)	28.931(4)	438.08
Nd	1.109	3.9021(3)	28.986(5)	441.35

TABLE 2
Cationic Ratios and Chemical Composition as Determined by EDS Analysis

Ln	Hg/Cu	Ba/Cu	*Ln*/Cu	(Hg + *Ln*)/Cu	(Ba + *Ln*)/Cu	Cation composition
Lu	0.75(5)	1.0(8)	0.76(7)	1.51(8)	1.8(1)	$Hg_{1.5(1)}Ba_{2.1(1)}Lu_{1.5(1)}Cu_{2.0(1)}$
Yb	0.76(8)	0.93(5)	0.64(8)	1.41(9)	1.6(1)	$Hg_{1.6(1)}Ba_{1.96(7)}Yb_{1.4(1)}Cu_{2.08(7)}$
Er	0.75(8)	0.97(8)	0.69(6)	1.45(12)	1.7(1)	$Hg_{1.54(8)}Ba_{1.98(9)}Er_{1.43(8)}Cu_{2.1(1)}$
Gd	0.85(6)	0.96(9)	0.63(6)	1.46(9)	1.6(1)	$Hg_{1.7(1)}Ba_{2.0(1)}Gd_{1.3(1)}Cu_{2.05(8)}$
Nd	0.92(9)	0.87(9)	0.63(5)	1.56(9)	1.5(1)	$Hg_{1.9(2)}Ba_{1.8(2)}Nd_{1.3(1)}Cu_{2.06(9)}$

As for the Ln_2CuO_4(9–11) system, the magnetic measurements could indicate that the rare earth and Cu moments behave as independent magnetic systems over a large temperature range; In the absence of information about the possible "antiferromagnetic" ordering of the Cu^{2+} moments at high temperature, we expect that the transition at T_L could be associated with an ordering of the Cu moments. However, more experiments are needed to study the magnetic properties of these materials as a function of the doping and to exclude the possibility of parasitic phases.

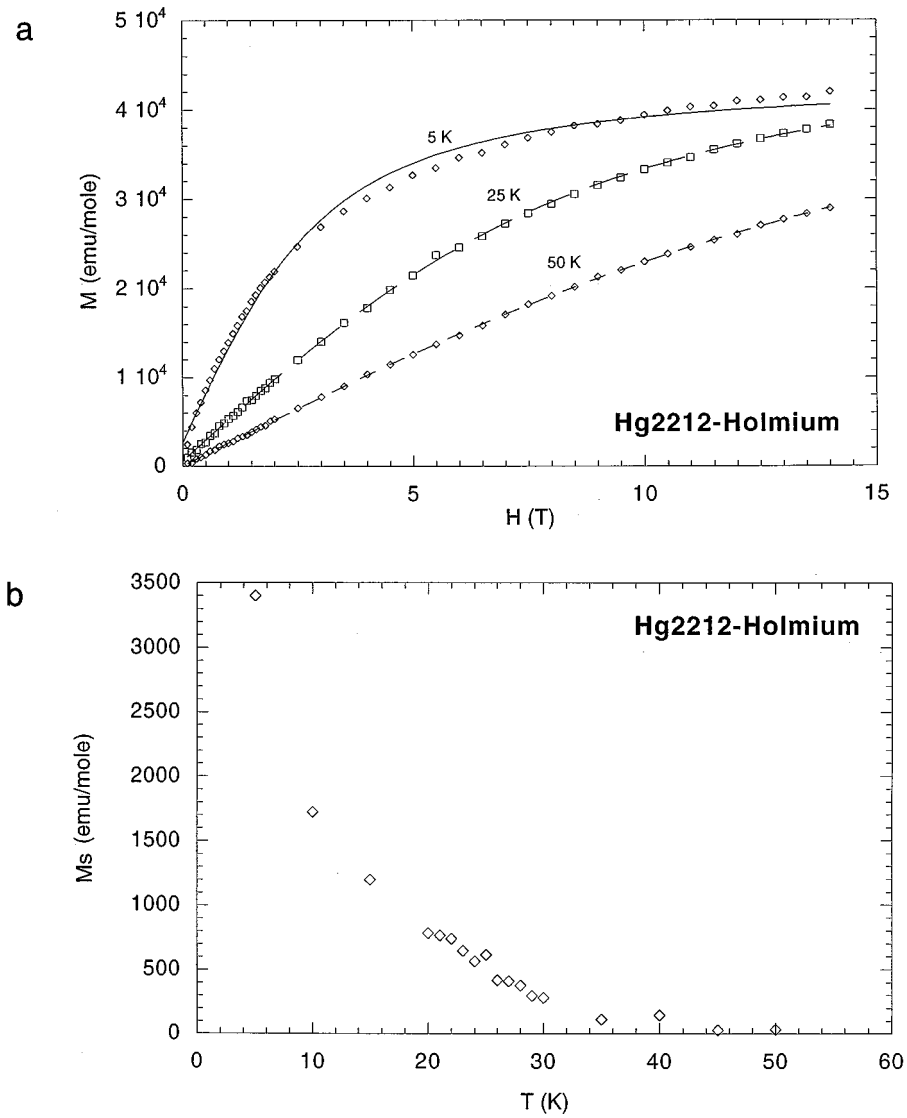

FIG. 6. (a) Magnetization of 2212-Ho sample for different temperatures (5–50 K). (b) Magnetization vs temperature for the 2212-Ho sample.

TABLE 3
Magnetic Properties of the Lanthanide Cations Ln^{3+} and the Synthesized 22*Ln*2 Samples

	Element	g	n_{eff} (calc.) free ion	n_{eff} (exp.) free ion	Total effective moment	θ (K)
$4f^0$	La	—	0,00	0,0		
$4f^1$	Ce	0,00	2,54	2,3–2,5		
$4f^2$	Pr	0,86	3,58	3,4–3,6		
$4f^3$	Nd	0,80	3,62	3,5–3,6	2,16	− 4.4
$4f^4$	Pm	0,73	2,68	—		
$4f^5$	Sm	0,29	0,84	1,5–1,6	≈ 0	
$4f^6$	Eu	—	0,00	3,4–3,6	≈ 0	
$4f^7$	Gd	2,00	7,94	7,8–8,0	5,21 ($T > 13$ K)	− 11.4
					7,64 ($T < 13$ K)	− 652.5
$4f^8$	Tb	1,50	9,72	9,4–9,6		
$4f^9$	Dy	1,33	10,63	10,4–10,5	10,68	− 6.6
$4f^{10}$	Ho	1,25	10,60	10,4–10,5	9,79 ($T < 25$ K)	
$4f^{11}$	Er	1,20	9,57	10,3–10,5	9,84	− 9.5
$4f^{12}$	Tm	1,17	7,63	9,4–9,6	7,11 ($T > 30$ K)	− 50.7
$4f^{13}$	Yb	1,14	4,50	4,4–4,9	2,47	− 4.4
$4f^{14}$	Lu	—	0,00	0,0		

CONCLUSION

The Hg-2212 structure seems to be extremely flexible due to its high ability to incorporate cations with such different ionic radius as lutetium or neodymium. New phases with Ln = Lu, Yb, Tm, Er, Ho, Dy, Gd, Eu, Sm, and Nd were synthesized for the first time. EDS analysis has determined that the rare earth cation can be incorporated into the Hg site up to some extent. The incorporation seems to be related to the ionic radius of the lanthanide since it is less pronounced when one reaches higher ionic radii. These phases are better described as $(Hg, Ln)_2Ba_2LnCu_2O_{8-\delta}$. In the case of Nd, another mechanism seems to occur and the replacement would take place on Ba-site as in $Hg_2(Ba, Ln)_2LnCu_2O_{8-\delta}$.

The Hg-2212 phases with rare earth cations with mixed $Ln^{+3,+4}$ valence were not found to form in our experimental conditions and lanthanum seems to have an ionic radius too high to be accommodated by this type of structure.

Magnetic anomalies which seem to be connected to the Cu spins have been found in the case of Sm, Eu, Dy, and Ho samples and are thought to be responsible for the rather large "ordering" temperatures observed. The respective contribution of the Cu and rare earth elements in the magnetic properties deserves further investigation.

Taking into account that the $Hg_2Ba_2(Y,Ca)Cu_2O_{8-\delta}$ compound exhibits superconductivity up to 70 K, these newly synthesized phases present a new field of activity.

ACKNOWLEDGMENTS

S.M.L. acknowledges a JNICT/PRAXIS XXI 3328/94 contract. P.T. thanks J. Voiron ("Louis Néel" Laboratory–CNRS, Grenoble) for the magnetization measurements. The authors thank INTAS (Grant 93-2483) and NATO (HTECH.LG 951022) for the partial support of this study.

REFERENCES

1. S. N. Putilin, I. Bryntse, and E. V. Antipov, *Mater. Res. Bull.* **26,** 1299–1307 (1991).
2. M. G. Rozova, M. V. Lobanov, E. M. Kopnin, M. L. Kobva, O. I. Lebedev, S. N. Putilin, and E. V. Antipov, *J. Alloys Compounds* **234,** 207–210 (1995).
3. N. R. Khasanova, I. Bryntse, and E. V. Antipov, *Physica C* **247,** 197–205 (1995).
4. S. N. Putilin, E. V. Antipov, O. Chmaissem, and M. Marezio, *Nature* **362,** 226–228 (1993).
5. A. Schilling, M. Cantoni, J. D. Guo, and H. R. Ott, *Nature* **363,** 56–58 (1993).
6. C. Martin, M. Hervieu, G. v. Tendeloo, F. Goutenoire, C. Michel, A. Maignan, and B. Raveau, *Solid State Commun.* **93,** 53–56 (1994).
7. P. G. Radaelli, M. Marezio, M. Perroux, S. de Brion, J. L. Tholence, Q. Huang, and A. Santoro, *Science* **265,** 380–383 (1994).
8. P. G. Radaelli, M. Marezio, J. L. Tholence, S. de Brion, A. Santoro, Q. Huang, J. J. Capponi, C. Chaillout, T. Krekels, and G. van Tendeloo, *Phys. Chem. Solids* **56,** 1471–1478 (1995)
9. M. Tovar, X. Obradors, F. Pérez, S. B. Oseroff, D. Chateigner, P. Bordet, J. Chenavas, P. Canfield, and Z. Fisk, *Magnet. Magnet. Mater.* **104–107,** 549–550 (1992).
10. M. Tovar, X. Obradors, F. Pérez, S. B. Oseroff, R. J. Duro, J. Rivas, D. Chateigner, P. Bordet, and J. Chenavas, *Phys. Rev. B* **45,** 4729 (1992).
11. X. Obradors, P. Visani, M. A. de la Torre, M. B. Maple, M. Tovar, F. Pérez, P. Bordet, J. Chenavas, and D. Chateigner, *Physica C* **213,** 81–87 (1993).